

## Supplementary Information

### Synthesis of thermoresponsive PNIPAm-*b*-PVP-*b*-PNIPAm hydrogels via aqueous RAFT polymerisation

Lauren E. Ball, Gabriela Garbonova, Rueben Pfukwa\* and Bert Klumperman\*

**Table S1.** RAFT mediated homopolymerisation of NVP for kinetic investigation and upscaled batches for subsequent PNIPAm chain extension kinetic experiments

Sample	$M_n^{\text{target}}$ (g/mol)	$\alpha$ (%) <sup>a</sup>	$M_n^{\text{theo b}}$ (g/mol)	$M_n^{\text{SEC c}}$ (g/mol)	$D^c$
PVP <sub>154</sub>	29 000	60	17 600	11 600	1.17
PVP <sub>165</sub>	28 300	66	18 800	18 100	1.18
PVP <sub>179</sub>	73 300	61	17 000	20 100	1.16
PVP <sub>242</sub>	67 900	40	27 400	25 500	1.20

a) Conversion determined via <sup>1</sup>H NMR spectroscopy, using the method described below.

b) Calculated using  $\alpha$

c) Determined via SEC using DMF as the mobile phase and PMMA calibration standards

**Table S2.** RAFT mediated chain extension of PVP macro-CTA samples in Table S1 with PNIPAm, for reaction parameter optimization and kinetic investigation

Entry	Sample composition	[R]:[I] <sup>a</sup>	Exp. Cond. <sup>b</sup>	$M_n^{\text{target}}$ ( $\times 10^3$ g/mol)	$\alpha$ (%) <sup>c</sup>	$M_n^{\text{theo d}}$ ( $\times 10^3$ g/mol)	$M_n^{\text{SEC e}}$ ( $\times 10^3$ g/mol)	$D^e$
1	A <sub>165</sub> -(B <sub>105</sub> ) <sub>2</sub>	1: 0.2	50 °C, 1h	42.6	98	42.2	42.7	2.39
2	A <sub>242</sub> -(B <sub>105</sub> ) <sub>2</sub>	1: 0.5	25 °C, 10min; 50 °C, 5 h	51.3	100	51.3	45.3	1.67
3	A <sub>242</sub> -(B <sub>105</sub> ) <sub>2</sub>	1: 0.5	30 °C, 20 h	51.1	100	51.1	53.8	1.56
4	A <sub>179</sub> -(B <sub>234</sub> ) <sub>2</sub>	1: 0.5	30 °C, 1 h	73.3	100	73.3	236.5	1.32
5	A <sub>179</sub> -(B <sub>234</sub> ) <sub>2</sub>	1: 0.2	30 °C, 0.5 h	73.3	99	72.8	327.9	1.30

a) Ratio of PVP macro-CTA to redox initiator pair, where A in the sample code refers to PVP homopolymers summarized in Table S1 and B refers to PNIPAm

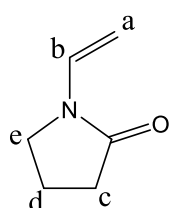
b) Experimental conditions used during the RAFT polymerisation. All reactions were conducted in PBS at 15 wt%.

c) Conversion determined via <sup>1</sup>H NMR spectroscopy, using DMF as an internal reference standard

d) Calculated using  $\alpha$

e) Determined via SEC using DMF as the mobile phase and PMMA calibration standards

### Conversion calculation for the kinetic investigation of RAFT mediated polymerisation of NVP:



a (4.4-4.3 ppm): Int. = 2.00  
b (7.0-6.9 ppm): Int. = 1.00  
c (2.4-2.35 ppm): Int. = 2.05  
d (2.14-2.05 ppm): Int. = 1.97  
e (3.52-3.47 ppm): Int. = 2.09

#### Calculating the correction factor at t<sub>0</sub>:

Integral average for vinyl protons =  $3.00/3 = 1$

Integral average for aliphatic protons =  $(2.05+1.97+2.09)/6 = 1.0183$

Correction factor = (vinyl)/(aliph.) =  $1/1.0183 = 0.981997$

#### Representative calculation for conversion at t<sub>0.5</sub>:

Integral average for 2 vinyl protons =  $3.04/3 = 1.013*2 = 2.026$

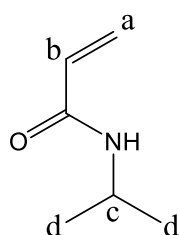
Corrected integral for **He** =  $2.026/0.981997 = 2.0631$

Total integral for **He**(NVP) and **He**(PVP) = 3.17

**He**(PVP) =  $3.17-2.0631 = 1.1069$

NVP conversion =  $1.1069/3.17*100 = 34.9 \%$

### Conversion calculation for the kinetic investigation of RAFT mediated polymerisation of NIPAm:



a (6.3-6.13 ppm)  
b (6.3-6.13, 5.75-5.71 ppm), total vinyl integral = 252.15  
c (4.02-3.95 ppm): Int. = 78.76  
d (1.18-1.15 ppm): Int. = 509.13

When using DMF as an internal standard a representative conversion calculation proceeds as follows:

Vinyl integral at t<sub>0</sub> =  $252.15/3 = 84.05$

Vinyl integral at t<sub>2</sub> =  $209.24/3 = 69.75$  therefore conversion at t<sub>2</sub> =  $(1-(69.75/84.05))*100 = 17.02 \%$

To completely avoid organic contaminants in the system, one can use a similar conversion calculation method as described for NVP, where the NIPAm protons (**Hc**) can be integrated against PNIPAm protons (**Hc**). This does have an error margin however as the PNIPAm protons overlap slightly with some PVP protons.

A representative calculation for this method at t<sub>2</sub>:

**Hc**(NIPAm) integral at t<sub>2</sub> = 67.34

**Hc**(PNIPAm+NIPAm) integral at t<sub>2</sub> = 78.98

**Hc**(PNIPAm) integral at t<sub>2</sub> =  $78.98-67.34 = 11.64$

NIPAm conversion =  $(11.64/78.98)*100 = 14.74 \%$

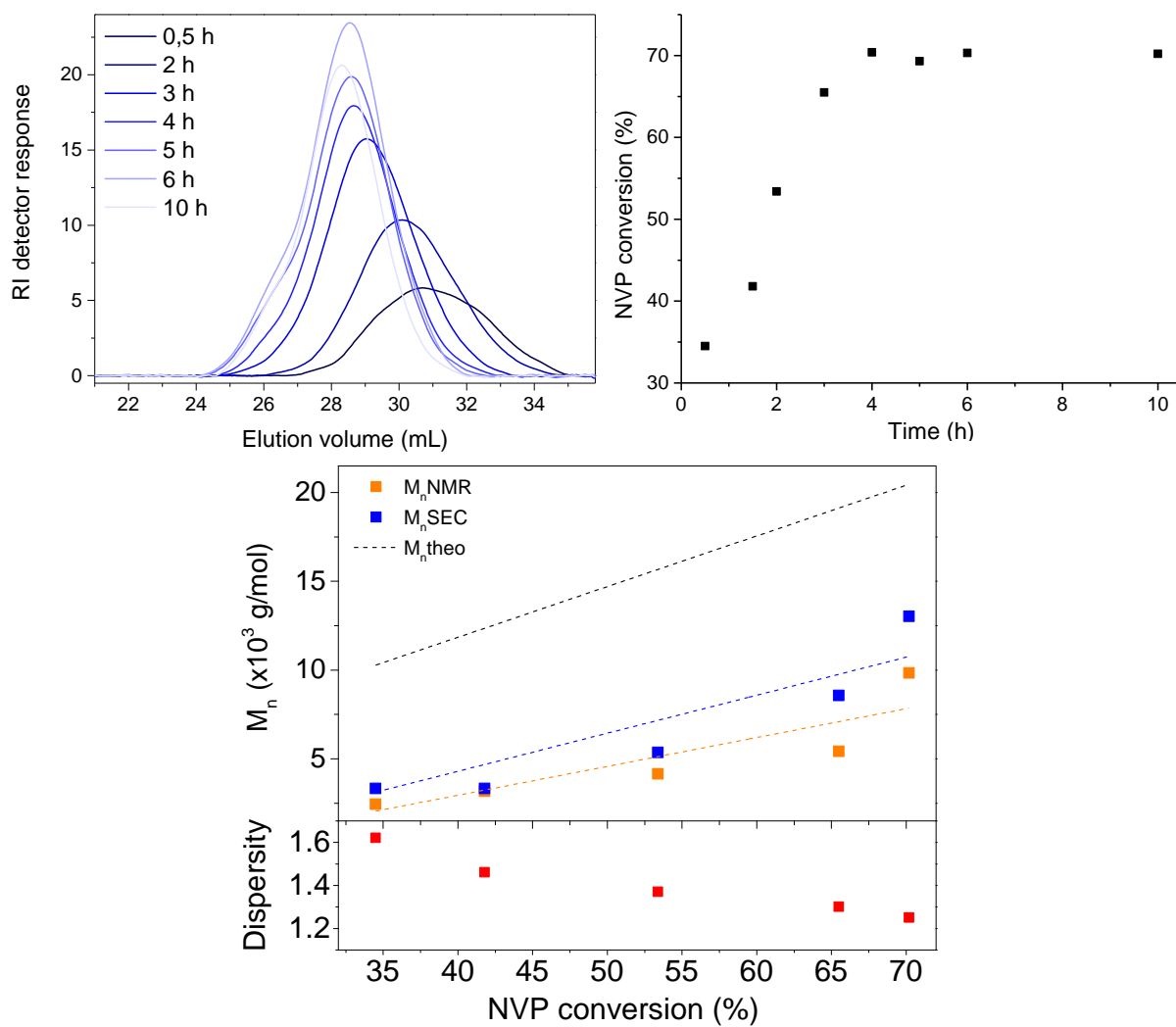


**Figure S1.** Kinetic analysis for the RAFT homopolymerisation of NVP. SEC analysis (top left), monomer conversion determined via <sup>1</sup>H NMR (top right) and M<sub>n</sub> and dispersity vs. NVP conversion (bottom).

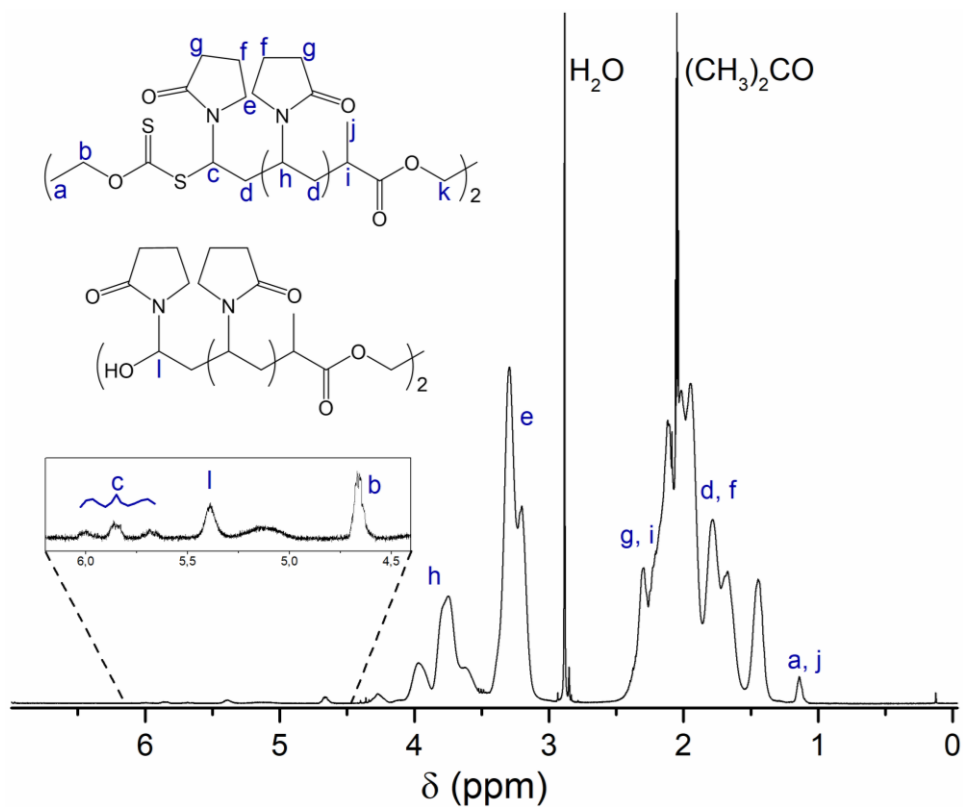


**Figure S2.** PVP<sub>154</sub>, dialyzed at ambient temperature, freeze dried and analysed via  $^1\text{H}$  NMR spectroscopy ( $(\text{CD}_3)_2\text{CO}$ ).

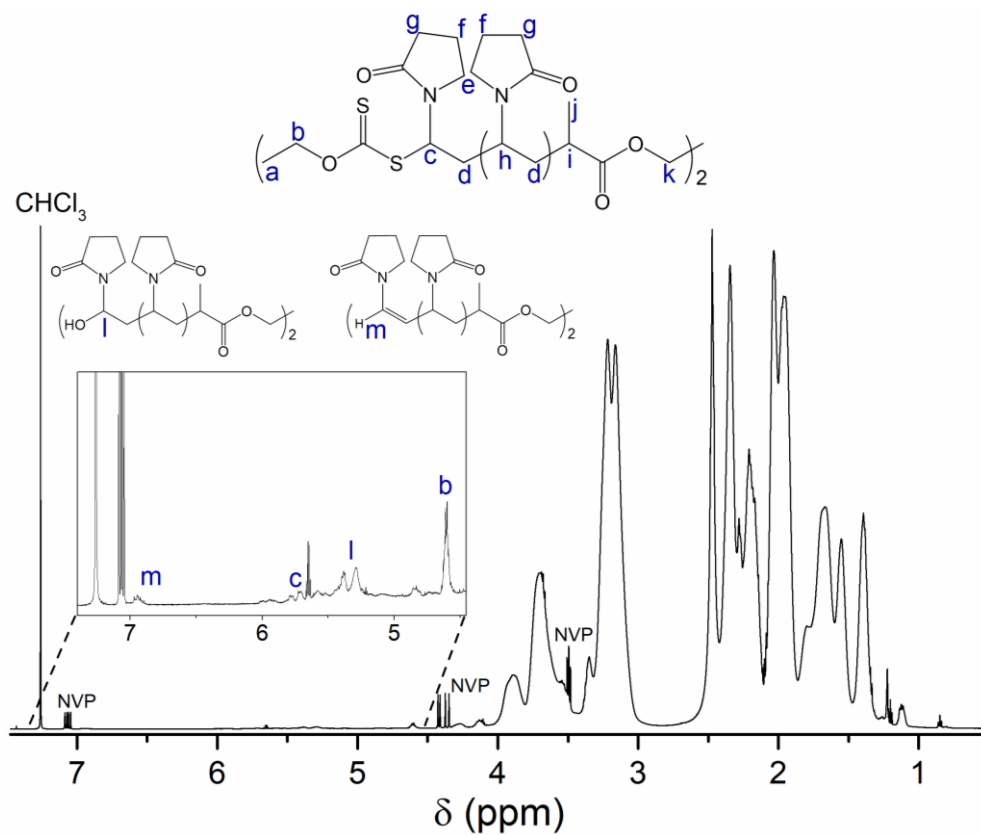


**Figure S3.** PVP<sub>165</sub>, dialyzed at ambient temperature, freeze dried, stored in sealed vessel at ambient temperature and analysed via  $^1\text{H}$  NMR spectroscopy ( $\text{CDCl}_3$ ).

Evidence of Z-group elimination can be observed in Figure S2 and S3, via both hydrolysis and thermolysis pathways, the former being the more predominant pathway, processes which can occur during polymerisation and storage. The hydrolysis of xanthate moieties from PVP chain ends has been reported previously and results in  $\omega$ -hydroxyl end-capped PVP, where the adjacent terminal NVP unit has a methine proton that can be observed between  $\sim$ 5.3-5.4 ppm (proton l, Figure S2, S3). These protons can be observed in the final kinetic sample and in the isolated and purified PVP, suggesting that this reaction could occur to some extent during the polymerisation and purification, both of which take place in water. The thermal lability of the Z-group at a PVP chain end also makes the xanthate moiety amenable to thermolysis, which creates unsaturated chain ends, identified as the proton at  $\sim$ 6.9 ppm (proton m, Figure S3).

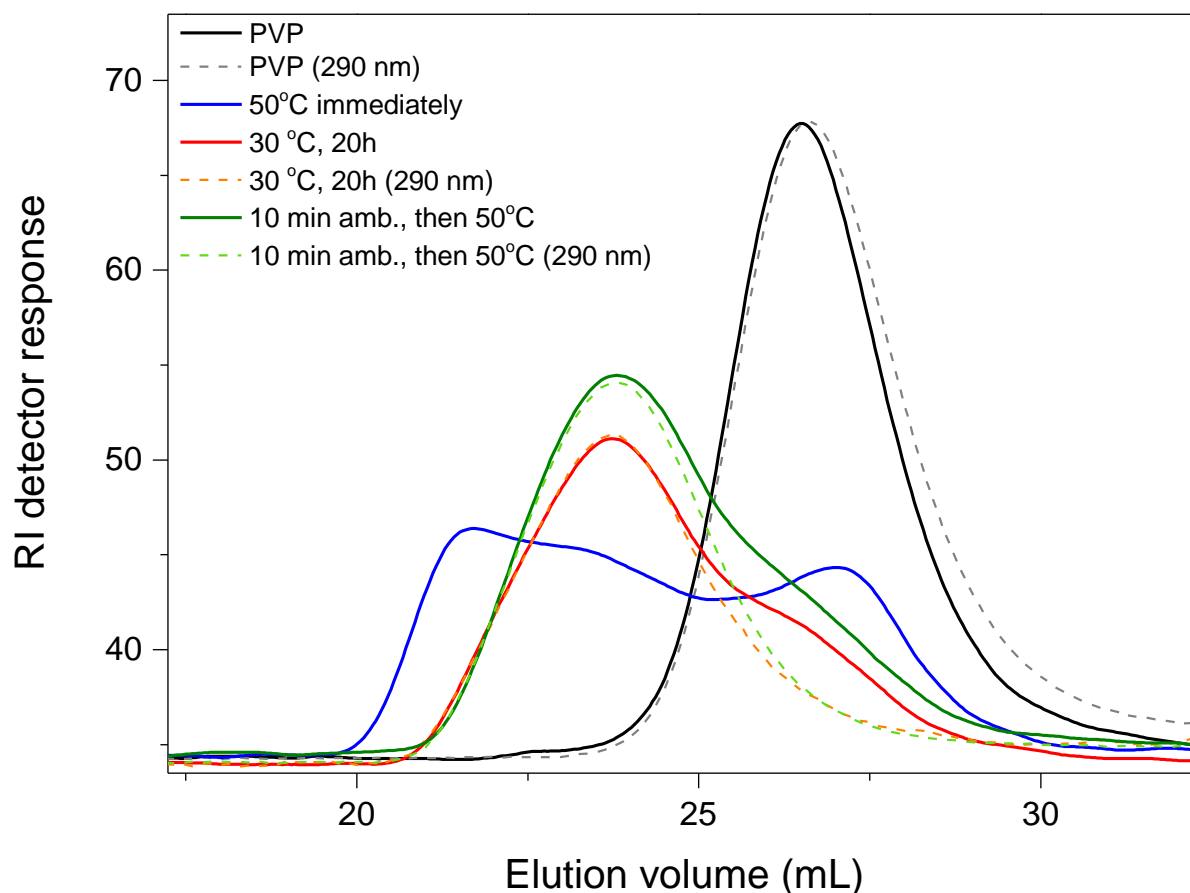


**Figure S4.** DMF SEC analysis for polymerisation temperature optimization study (Table S2, entry 1, 2, 3). RI detector response is represented by solid lines, while UV detector response (290 nm) is represented by dashed lines.

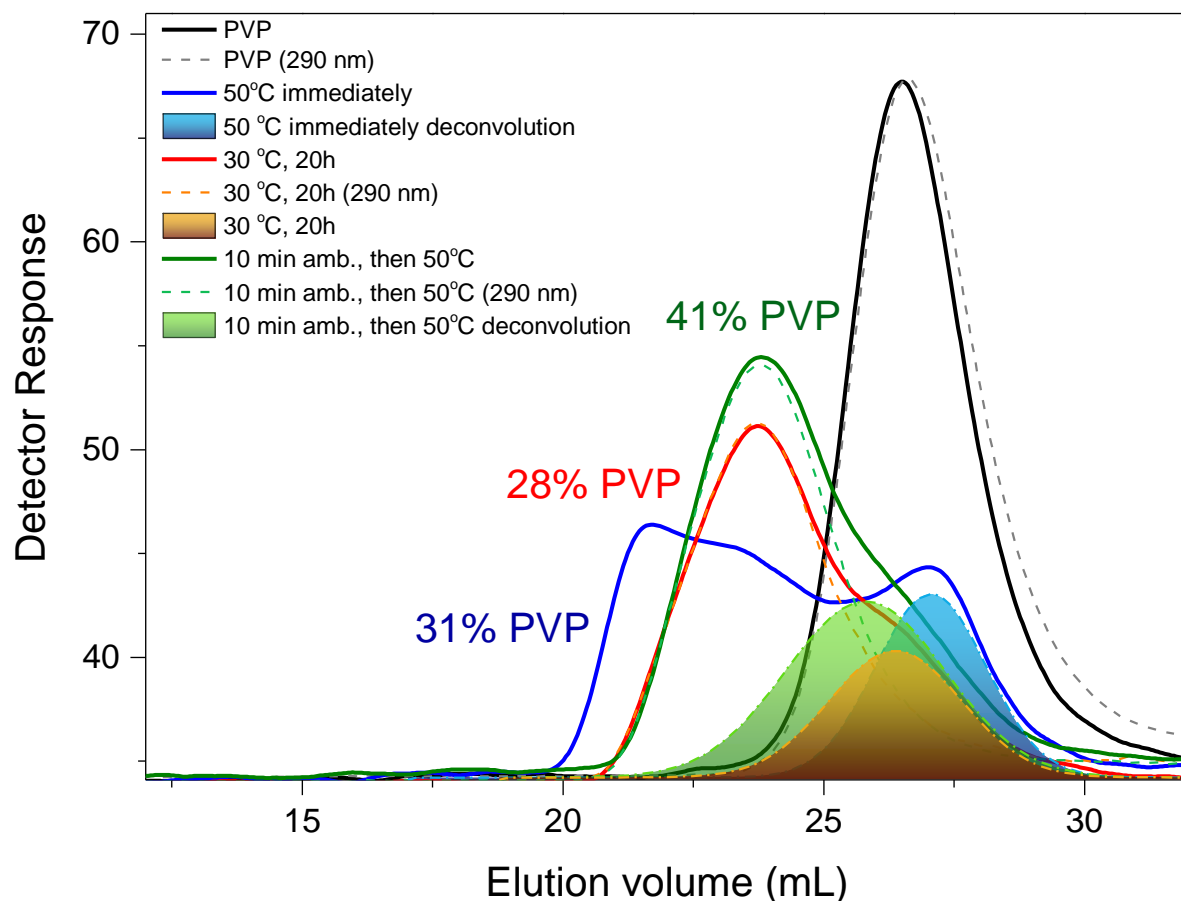


**Figure S5.** Deconvoluted DMF SEC data for polymerisation temperature optimization study (Table S2, entry 1, 2, 3). RI detector response is represented by solid lines, the UV detector response by dashed lines, while the filled in curves represent the fitted data from the deconvolution of PNIPAm-*b*-PVP-*b*-PNIPAm molecular weight distributions. These deconvoluted peaks are proposed to represent dead PVP chains.

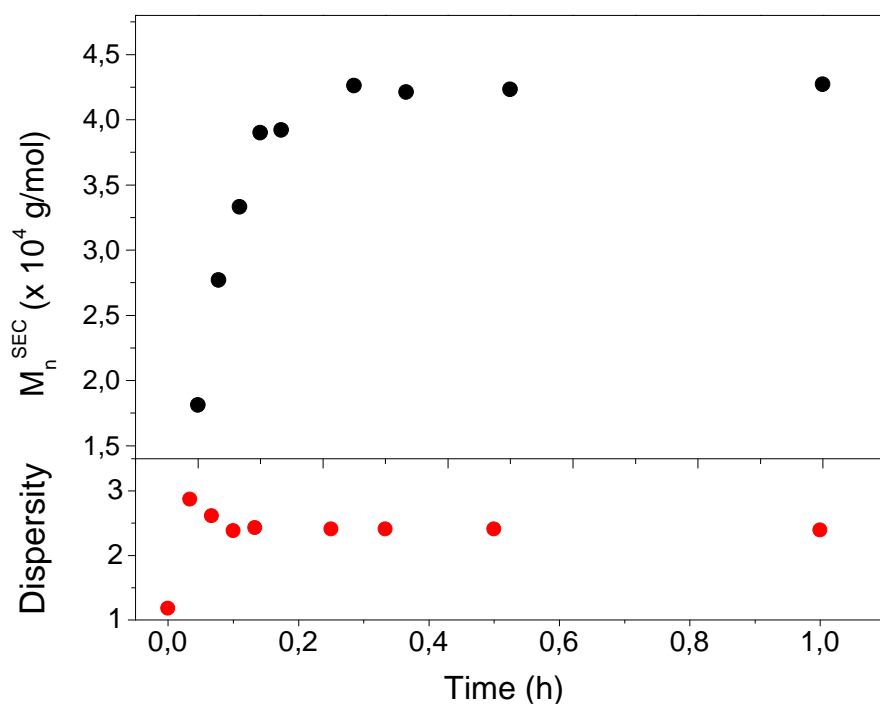


**Figure S6.** Kinetic analysis of the RAFT mediated chain extension of PVP<sub>165</sub> (Table S2, entry 1) with PNIPAm, where the reaction mixture was brought to 50 °C immediately after Na<sub>2</sub>SO<sub>3</sub> addition.  $M_n^{SEC}$  determined via DMF SEC using PMMA calibration standards.

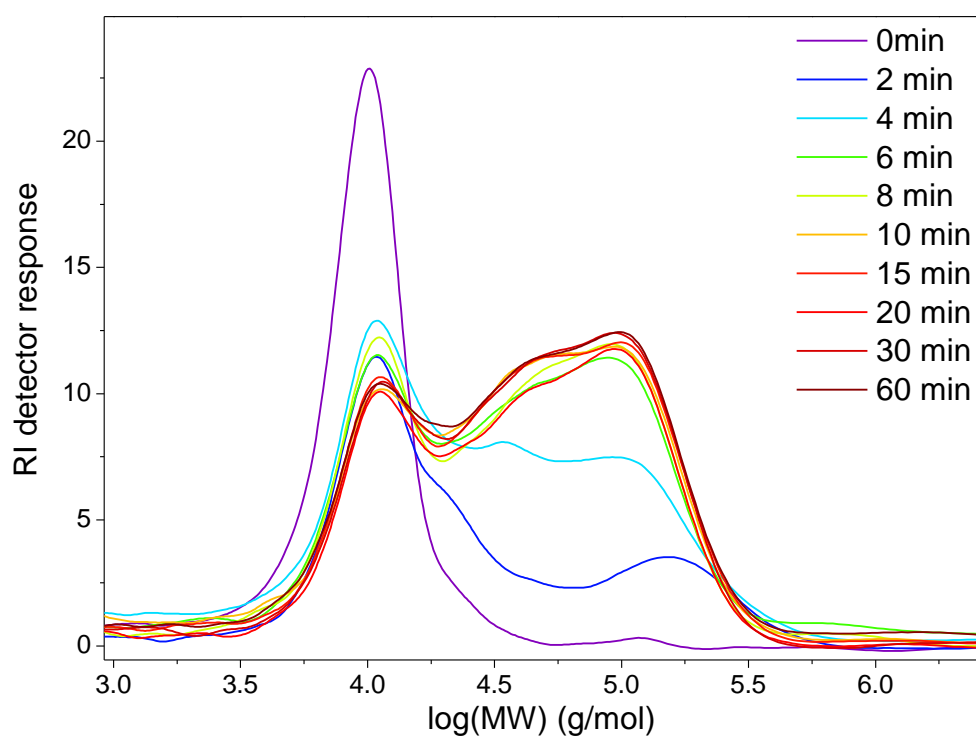


**Figure S7.** Kinetic analysis of the RAFT mediated chain extension of PVP<sub>165</sub> (Table S2, entry 1) with PNIPAm, where the reaction mixture was brought to 50 °C immediately after Na<sub>2</sub>SO<sub>3</sub> addition. Molecular weight distributions obtained via DMF SEC using PMMA calibration standards.

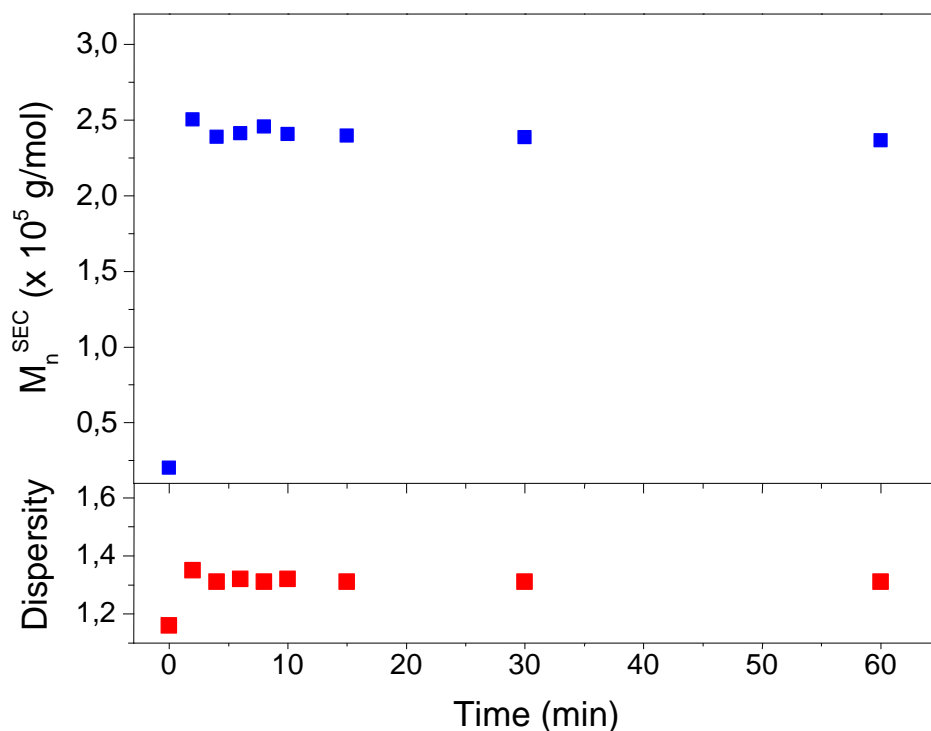


**Figure S8.** Kinetic analysis of the RAFT mediated chain extension of PVP<sub>179</sub> (Table S2, entry 4) with PNIPAm, where the polymerisation proceeded at 30 °C throughout, but with higher radical concentration.  $M_n^{SEC}$  determined via DMF SEC using PMMA calibration standards.

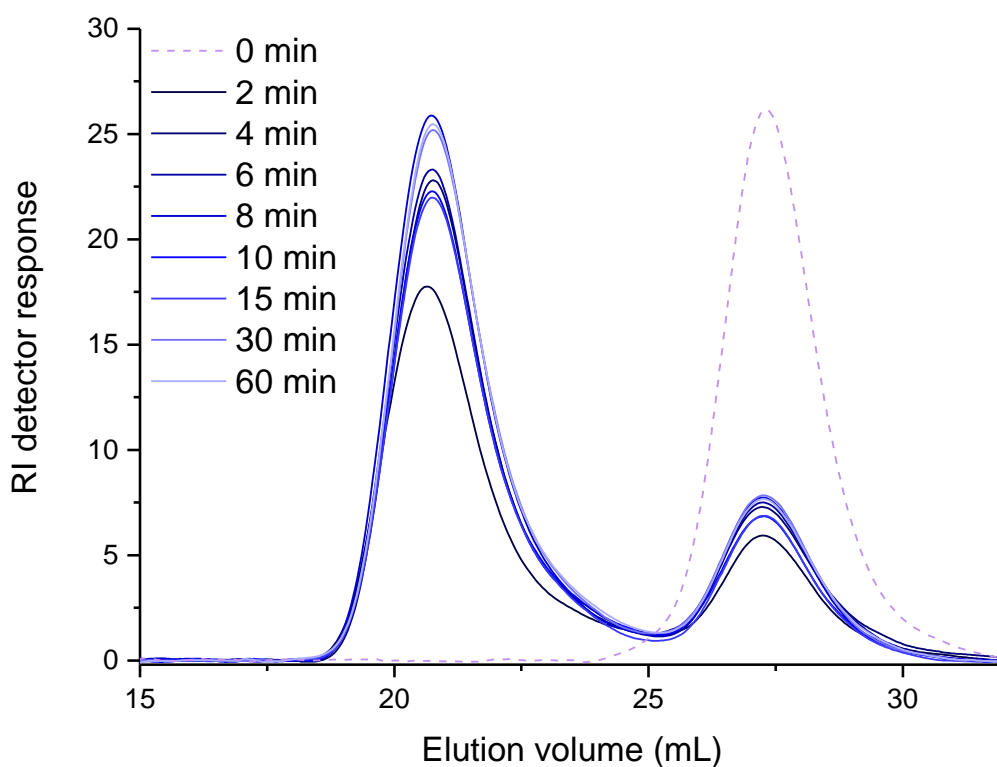


**Figure S9.** Kinetic analysis of the RAFT mediated chain extension of PVP<sub>179</sub> (Table S2, entry 4) with PNIPAm, where the polymerisation proceeded at 30 °C throughout, but with higher radical concentration. Molecular weight distributions obtained via DMF SEC using PMMA calibration standards.



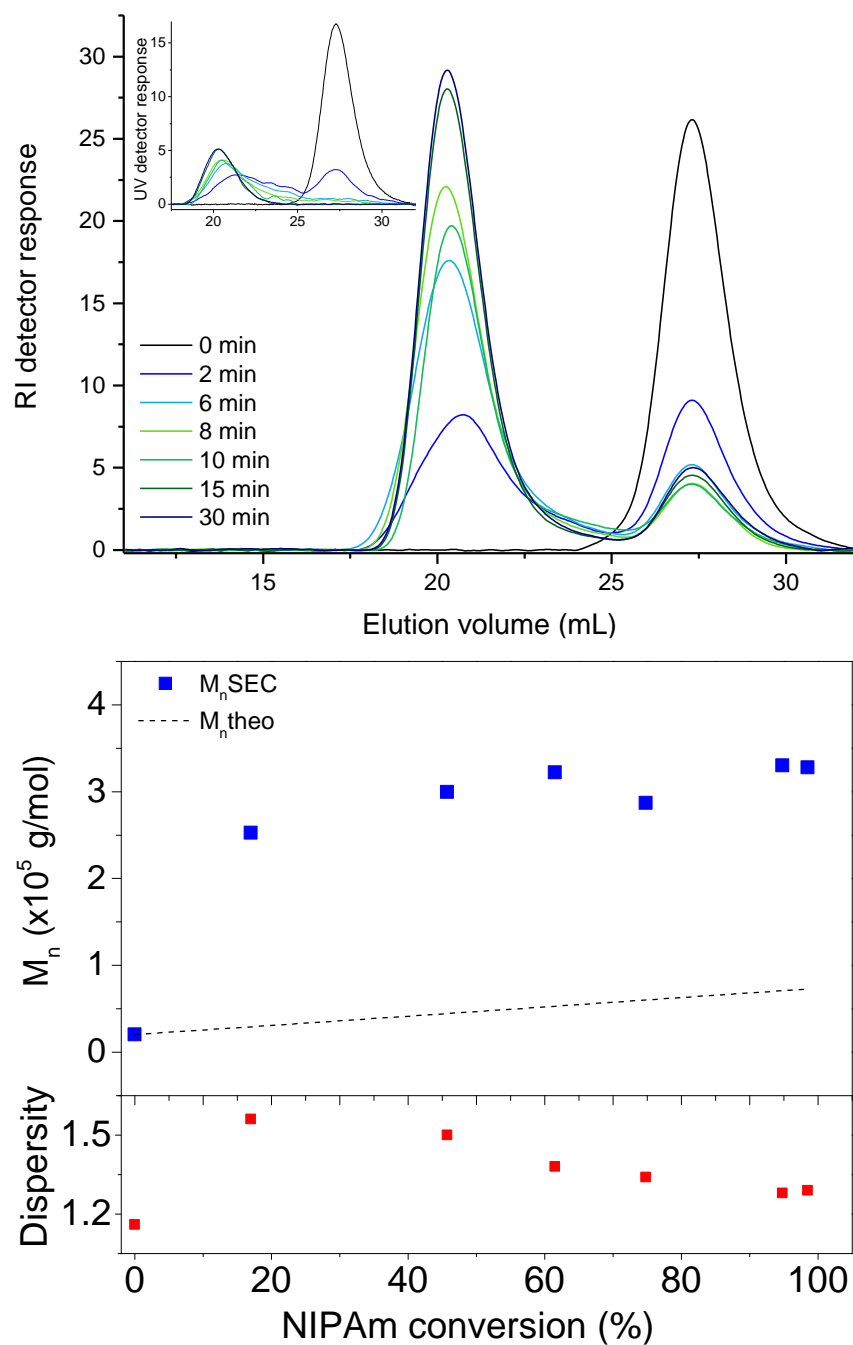


**Figure S10.** Kinetic analysis of the RAFT mediated chain extension of PVP<sub>179</sub> (Table S2, entry 5) with PNIPAm, where the polymerisation proceeded at 30 °C throughout, but with lower radical concentration. Molecular weight distributions obtained via DMF SEC using PMMA calibration standards, with the UV detector response given in the inset (top) and  $M_n$ /Dispersity vs NIPAM conversion (bottom).

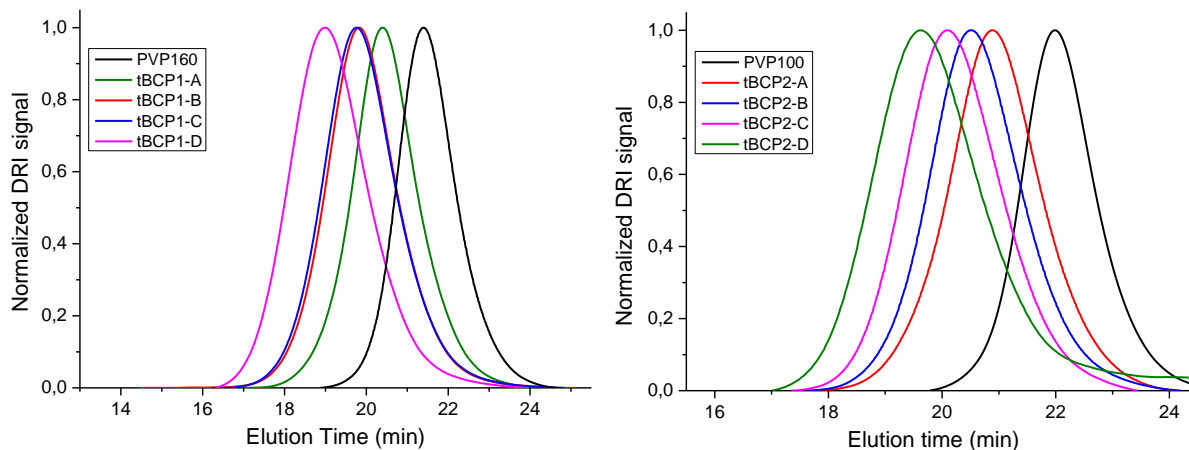


**Figure S11.** SEC analysis for the tBCP1 and tBCP2 series via DMF SEC using PMMA calibration standards.

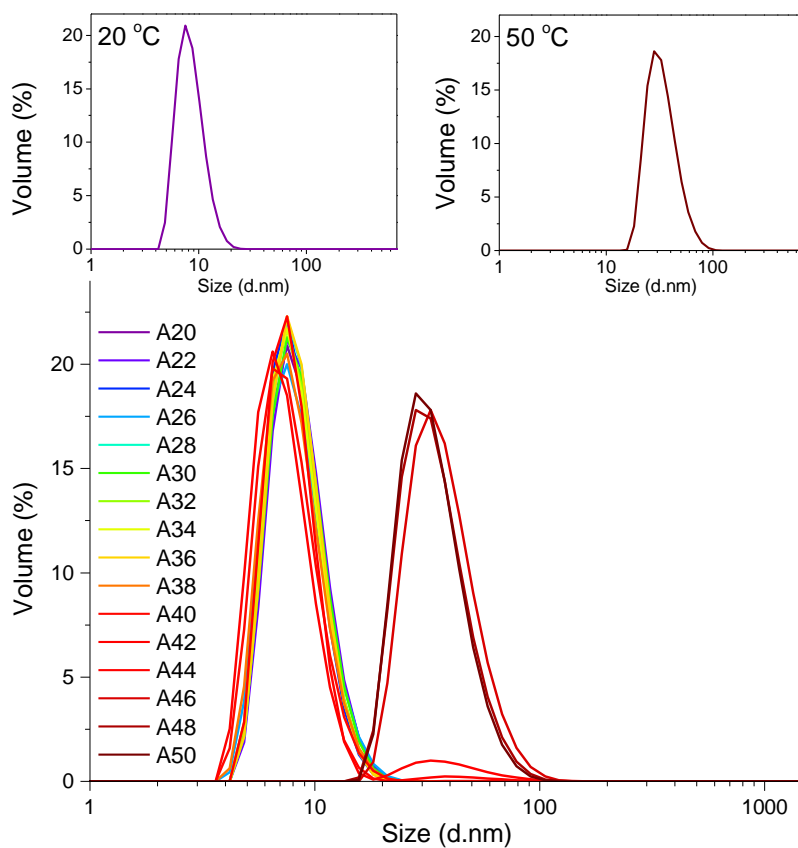


**Figure S12.** Variable temperature DLS analysis for a dilute aqueous solution of tBCP1-A.

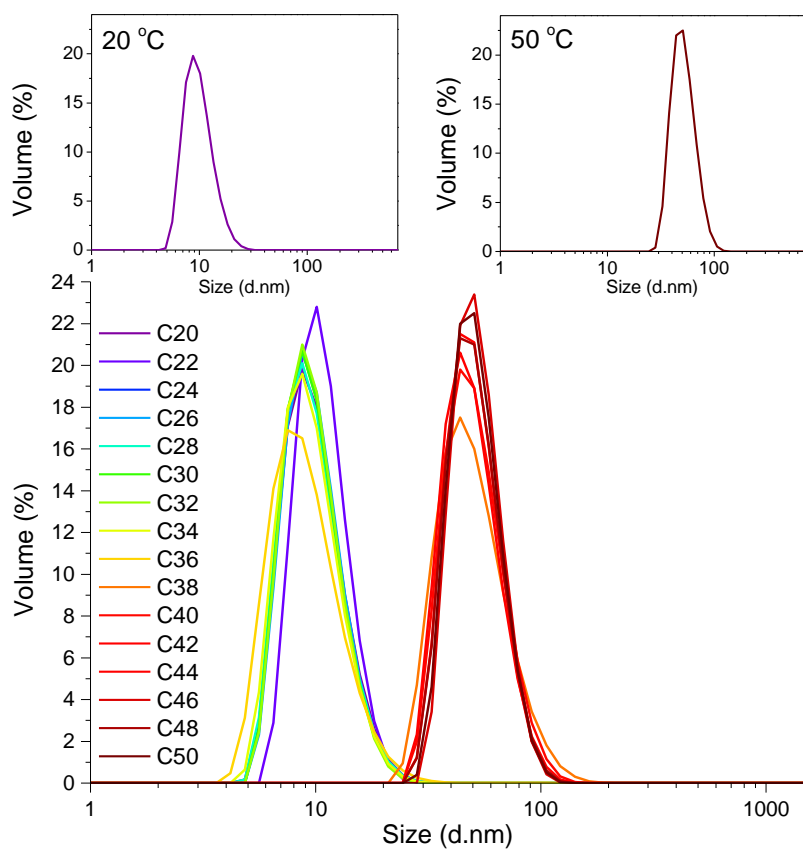


**Figure S13.** Variable temperature DLS analysis for a dilute aqueous solution of tBCP1-C.

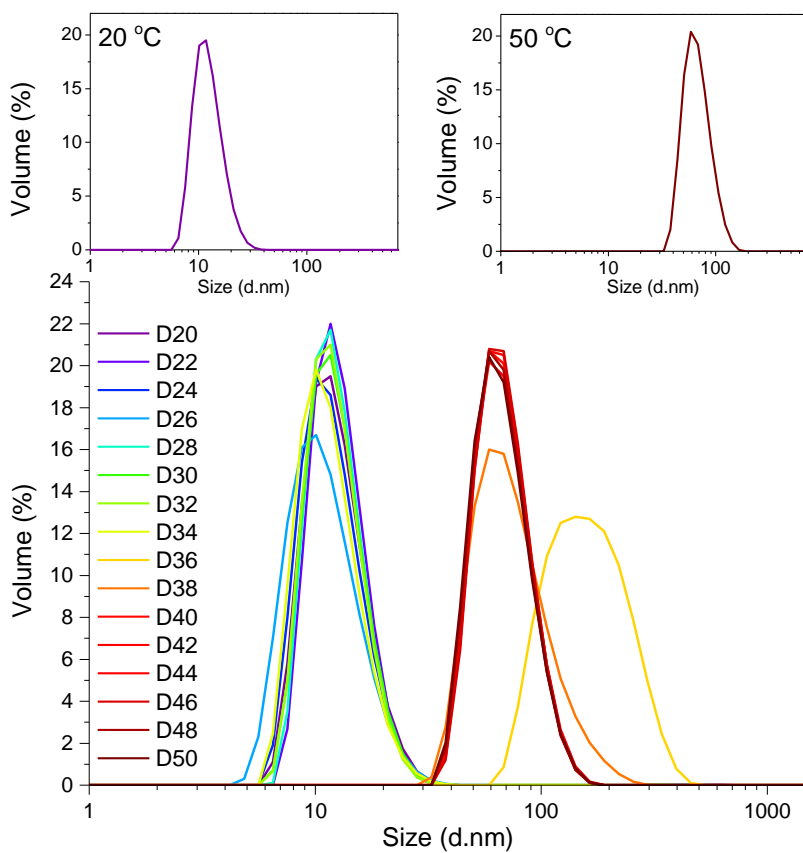


**Figure S14.** Variable temperature DLS analysis for a dilute aqueous solution of tBCP1-D.

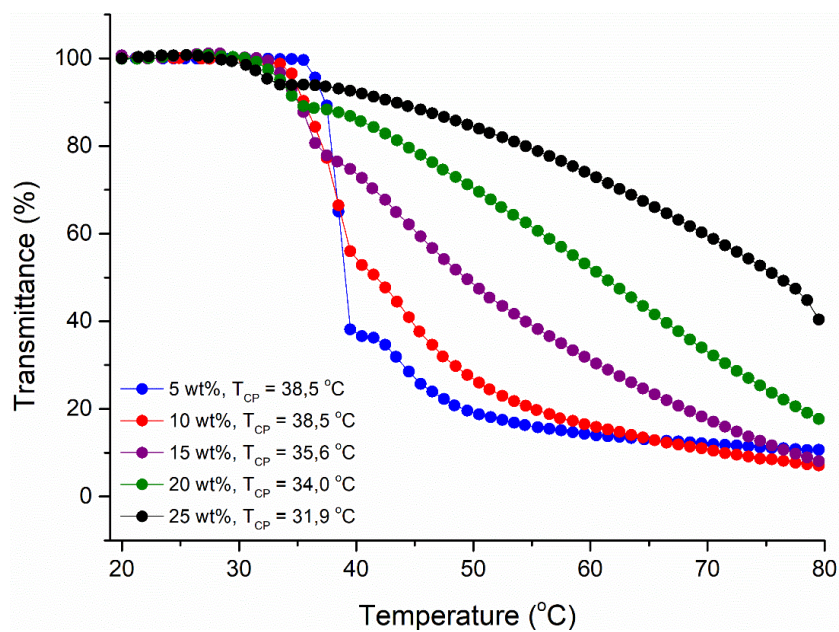


**Figure S15.** Turbidimetry analysis for the effect of tBCP1-D concentration on the  $T_{CP}$ .

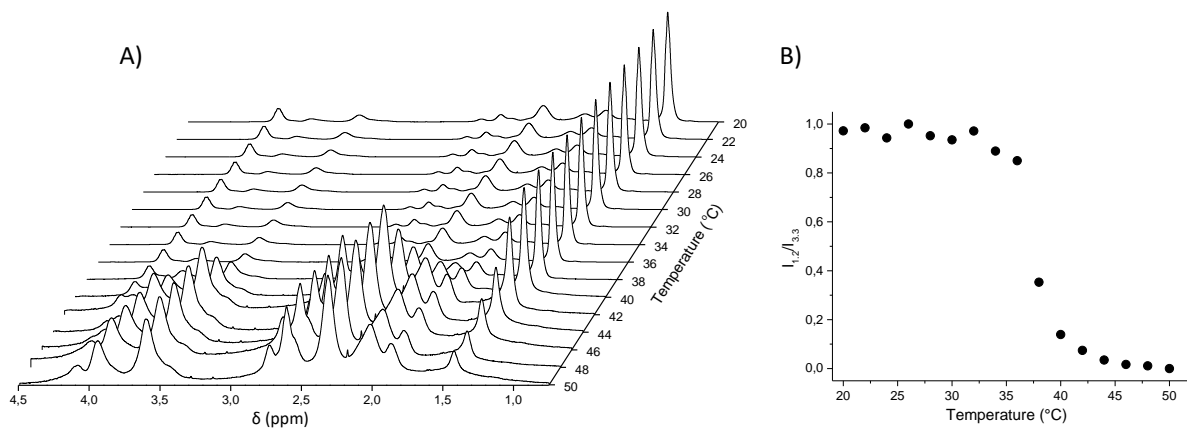


**Figure S16.** Temperature dependent  $^1\text{H}$  NMR spectra of tBCP1-D indicating the pendent methyl signals from PNIPAm. (b) Plots of normalized NMR signal intensity ratio  $I_{1,2}/I_{3,3}$  for tBCP1-D in  $\text{D}_2\text{O}$  as a function of temperature, where  $I_{1,2}$  and  $I_{3,3}$  are NMR signal intensities at 1.2 and 3.3 ppm assigned to PNIPAm and PVP, respectively.